Properties of localization in silicon-based lattice periodicity breaking photonic crystal waveguides

Yuquan Wu, Xiaofei Wang, Yuanbin Wu, Yufang Wang, Guoquan Zhang, Wande Fan, and Xuewei Cao'

Citation: AIP Advances **3**, 112107 (2013); doi: 10.1063/1.4830280
View online: http://dx.doi.org/10.1063/1.4830280
View Table of Contents: http://aip.scitation.org/toc/adv/3/11
Published by the American Institute of Physics

Properties of localization in silicon-based lattice periodicity breaking photonic crystal waveguides

Yuquan Wu,[1] Xiaofei Wang,[1] Yuanbin Wu,[1,2,3] Yufang Wang,[1]
Guoquan Zhang,[1] Wande Fan,[1] and Xuewei Cao[1,a]
[1]*School of Physics, Nankai University, Tianjin, 300071, P. R. China*
[2]*Dip. di Fisica, Università di Roma "La Sapienza", Piazzale Aldo Moro 5, I-00185 Roma, Italy*
[3]*EDSFA, Université de Nice Sophia Antipolis, 06103 Nice, France*

(Received 17 May 2013; accepted 30 October 2013; published online 7 November 2013)

The light localization effects in silicon photonic crystal cavities at different disorder degrees have been studied using the finite difference time domain (FDTD) method in this paper. Numerical results showed that localization occurs and enhancement can be gained in the region of the cavity under certain conditions. The stabilities of the localization effects due to the structural perturbations have been investigated too. Detailed studies showed that when the degree of structural disorder is small(about 10%), the localization effects are stable, the maximum enhancement factor can reach 16.5 for incident wavelength of 785 nm and 23 for 850 nm in the cavity, with the degree of disorder about 8%. The equivalent diameter of the localized spot is almost constant at different disorder degrees, approximating to $\lambda/7$, which turned out to be independent on the structural perturbation. [http://dx.doi.org/10.1063/1.4830280]

I. INTRODUCTION

Due to its attractive optical properties in controlling and manipulating the flow of light, a substantial amount of work has been devoted in the past few years to understand transport, wave-scattering and localization phenomena in nanophotonic crystals.[1–5] The existence of photonic band gap (PBG),[6,7] which is an unique feature of photonic crystals, has given rise to distinct optical phenomena such as inhibition of spontaneous emission,[8–11] high-reflecting omni-directional mirrors[12] and low-loss-waveguiding.[13–16] Such activities have unveiled broad application prospects in technological and engineering fields of photonics and optoelectronics industry.[17,18] Higher dimensional photonic crystals are of great interest for both fundamental and applied research, and the two dimensional ones have already found commercial applications, in the form of photonic crystal fibers,[19] which use a microscale structure to confine light with radically different characteristics compared to conventional optical fibers for applications in nonlinear devices and guiding exotic wavelengths.[20,21] After random structures have been introduced, more fascinating analogies between the behavior of electronic and optical waves were observed, such as disorder-induced Anderson light localization,[5,22–29] the photonic Hall effect,[30] optical magneto resistance,[31] universal conductance fluctuations of light waves,[32] and optical negative temperature coefficient resistance.[33] The breaking of the structural uniformity and periodicity is in fact providing a convenient path to confine light dispersion in transverse section and forming field localization.[34,35] However, the irregularity of random structures have made them irreproducible and of very limited appeal in actual manufacturing, more detailed investigation on the functioning mechanism is imperative and some kind of specific design rules should be developed for us to conceive, explore, and fabricate.

[a]Author to whom correspondence should be addressed. Electronic mail: xwcao@nankai.edu.cn.

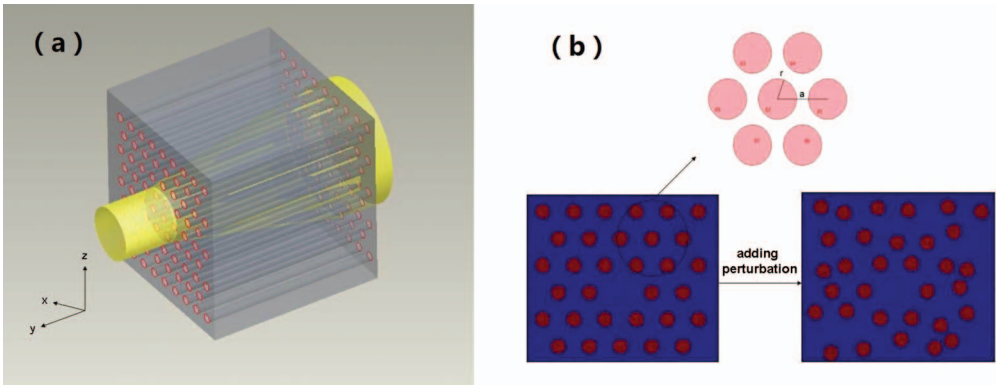

FIG. 1. Schematic of the structure geometry. (a) The coordinates of the system and the propagating direction of the incident light. (b) Index profile in the transverse section of the nanostructure (homogeneous and with displacement perturbation). r is the radius of the air hole and a is the lattice constant. E1 ~ E7 is the sequence number of the seven holes inside the enlarged area.

In this paper, we are focusing on a very limited area inside a random-structured nanophotonic crystal in order to study the local effect of breaking the structural spatial periodicity. We modeled a nanostructure consisting of a hexagonal lattice of straight air holes distributed spatial periodically in a silicon cuboid, a cavity was formed by a missing hole in the center. Detailed simulation have been carried out by using the finite difference time domain method (FDTD) and the properties as well as the affecting factors of the light confinement in the structure have been studied by analyzing the numerical results.[36] Considering the techniques of actual fabrication and the electrochemical etching, there are many restrictions to make a rigorous regular nanostructure. So the effects of light confinement have also been studied when structural perturbations have been added. According to our results it has turned out that when the degree of structural disorder is small (<5%), the localization effects are comparable to that in the regular photonic crystals with a cavity. When the disorder degree was increased, the maximum enhancement was gained inside the cavity. So this structure can be used to provide additional enhancement to raise the luminescence efficiency of silicon-based photonic crystals besides the effects of enhanced Raman scattering from single silicon nanowire[37] and SERS.[38,39] When the degree of disorder is over 10%, the enhancement is even smaller than that in the regular photonic crystals.

II. MODEL AND CALCULATION

The coordinates of the system and the propagating direction of the incident wave (parallel to the y axis) are described in Figure 1(a). Figure 1(b) is a schematic of the transverse section of the cuboid with r as the radius of the hole and a as the lattice constant, L is the longitudinal length of the structure calculated in the simulation. We chose the radius of the hole as $r = m\lambda/64$ and the lattice constant as $a = i\lambda/8n + 2r$, (m and i are integers),[39] in which λ is the wavelength of the incident light, and n is the refractive index of silicon.[40]

We solved the Maxwell equations by the FDTD algorithm and calculated the distributions of the electromagnetic field in transverse sections at different y values vertical to the propagating direction, $I_{cs}(x, y, z)$ is defined as the energy intensity at point (x, y, z) in the transverse section. The unitary intensity distribution was defined as $I(x, y, z) = I_{cs}(x, y, z)/I_0$, with I_0 the average intensity of the incident light, since the initial conditions can be chosen arbitrarily.

In the study of disordered structures, we keep the cavity steady to gain enhancement of the emergent light by fixing the position of its surrounding six air holes while adding positional disorder to the others, as shown in Figure 1(b). The degree of disorder has been defined as $W = p/a$, while p is the maximum displacement. The values of the unitary intensity distribution $\overline{I}_R(x, y, z)$ are calculated based on the simulation results. Since the unitary intensity distribution can be Gaussian fitted, the equivalent diameter of the light spot D has been defined as the full width at half-maximum

(FWHM) of the Gaussian fitting, and the enhancement factor $G = \overline{I}_s / I_0$ ($\overline{I}_s$ is the average values of $\overline{I}_R(x, y, z)$.

III. RESULTS AND DISCUSSION

During the light propagation in the porous medium, scattering and refraction occurs at the inside interfaces. Supposing n_1, n_2 are the dielectric constants of dielectric material A and B, k_1, k_1', k_2 are the incident, reflected and refracted wave vector of the plane wave source, in the form of plane wave, respectively. E_1, E_1', E_2 are the electric field intensity of the incident, reflected and refracted wave. x-y plane is the interface plane. Then in the form of plane wave, we have:

$$E_1 = E_{10} \exp[i(k_1 \cdot r - \omega t)] \tag{1}$$

$$E_1' = E_{10}' \exp[i(k_1' \cdot r - \omega t)] \tag{2}$$

$$E_2 = E_{20} \exp[i(k_2 \cdot r - \omega t)] \tag{3}$$

Considering the boundary relation, we have:

$$k_{1x} = k_{1x}' = k_{2x}, \ k_{1y} = k_{1y}' = k_{2y} = 0$$

Let $\theta_1, \theta_1', \theta_2$ be the incident, reflecting and refracting angle, respectively. Then we have:

$$\sin\theta_1 = \frac{k_{1x}}{k_1}, \ \sin\theta_1' = \frac{k_{1x}'}{k_1'}, \ \sin\theta_2 = \frac{k_{2x}}{k_2},$$

From $k_1 = \frac{n_1\omega}{c}$, $k_1' = \frac{n_1\omega}{c}$, $k_2 = \frac{n_2\omega}{c}$, we can get:

$$\sin\theta_1 = \sin\theta_1', n_1 \sin\theta_1 = n_2 \sin\theta_2 \tag{4}$$

The z-component of the refracted wave vector

$$k_{2z} = \sqrt{k_2^2 - k_{2x}^2} = \frac{\omega n_1}{c}\sqrt{\left(\frac{n_2}{n_1}\right)^2 - \sin^2\theta_1} = \frac{2\pi}{\lambda}\sqrt{n_{21}^2 - \sin^2\theta_1} \tag{5}$$

λ is the wavelength of the propagating wave.

Considering that k_{2z} could be an imaginary number, rewrite it in the following form:

$$i\chi = \frac{2\pi}{\lambda}\sqrt{n_{21}^2 - \sin^2\theta_1} = i\frac{2\pi}{\lambda}\sqrt{\sin^2\theta_1 - \sin^2\theta_c}$$

$$\chi = \frac{2\pi}{\lambda}\sqrt{\sin^2\theta_1 - \sin^2\theta_c} \tag{6}$$

Combine Eq. (6) with Eq. (3), we have the expression of the wave propagation in dielectric material B:

$$E_2 = E_{20} e^{-\chi z} \exp[i(k_{2x}x - \omega t)] \tag{7}$$

Eq. (7) indicates that the refracted wave decays exponentially in the z direction, which is called the evanescent wave, it's effective penetration depth is defined as below:

$$d_z = \frac{1}{\chi} = \frac{\lambda_1}{2\pi}\frac{1}{\sqrt{\sin^2\theta_1 - n_{21}^2}} \tag{8}$$

Combine Eq. (8) with our simulation parameters, when the 785 nm and 850 nm plane waves propagate in our modeled porous silicon material, the effective penetration depth of the evanescent wave is comparable to our cavity size, and its interference enhancement occurs inside the cavity area in all probability, which will contribute to the energy intensity enhancement.

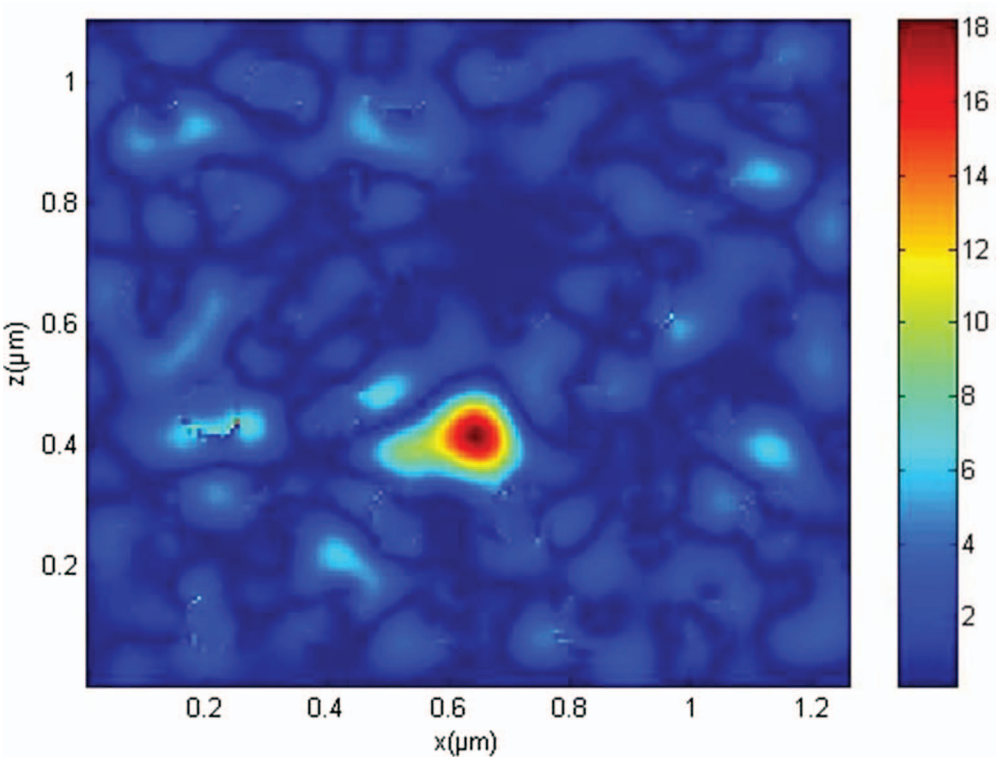

FIG. 2. The unitary intensity distribution in the transverse section close to the output plane of the regular nanostructure with $r = 49$ *nm*, $a = 204$ *nm*, and $L = 3\lambda$. The wavelength of the incident light is $\lambda = 785$ *nm*. The color bar shows the enhancement factor of the energy flux density.

Figure 2 shows the unitary intensity distribution in the cross section close to the output plane in a homogeneous nanostructure with the radius of the hole $r = 49$ *nm*, the lattice constant $a = 204$ *nm*, and a thickness of the structure $L = 3\lambda = 2355$ *nm*. The wavelength of the incident light is 785 *nm*. It is easy to conclude that the localization occurs and enhancement can be gained in the cavity in this case. Compared to the energy flux density of the incident light, the enhancement factor can reach 15 in the cavity.

Figure 3 shows the position distribution of the light spot along the direction of light propagation. The position of the light spot is defined as the position of the point with the maximum energy density in the spot, in which the spot's line width is ignored. As shown in Fig. 3(a), most of the light spots are located in a columnar region. In Fig. 3(b), these light spots are bounded within a 200 nm- diameter circle, which overlapped the cavity. Repeated calculations have shown that the light spots are always located in this region. Figure 4 shows that the equivalent diameter of the light spot is proportional to the incident wavelength, approximating to $\lambda/7$, which is comparable to $\lambda/2n$.

Furthermore, the localization effects in structures with different disorder degrees have been investigated. The perturbations have been added to the nanostructure as shown in Fig. 1(b). Figure 5 showed the emergent energy enhancements at different degrees of disorder at two incident wavelengths: (a) 785 *nm* and (b) 850 *nm*. $i = 2$ and $m = 4$ have been chosen, respectively. We chose the structure parameters as $r = 49$ *nm*, $a = 204$ *nm* and $L = 2355$ *nm* for incident light of *785nm*, and $r = 53$ *nm*, $a = 222$ *nm* and $L = 2550$ *nm* for incident light of 850nm. As shown in Figure 5, the effects of the disorder degree on the enhancement of the energy flux density are similar at the two incident wavelengths. When the degree of structural disorder is small ($< 5\%$), the enhancement is similar to that in the sample with regular structure. When the disorder degree is large (about 10% - 23%), the enhancement factors are reduced, which are about 10 for 785 nm and 15 for 850 nm, compared to the energy flux density of the incident light. When the degree of the

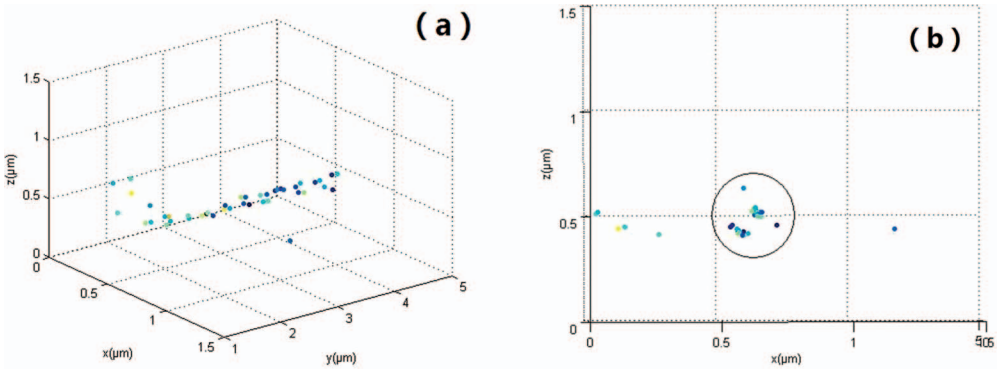

FIG. 3. The position distribution of the localized light spot along the direction of the propagating light. (a) The three-dimensional position distribution of the light spot in the sample; (b) A two-dimensional vertical view of spot position distribution in x-z plane.

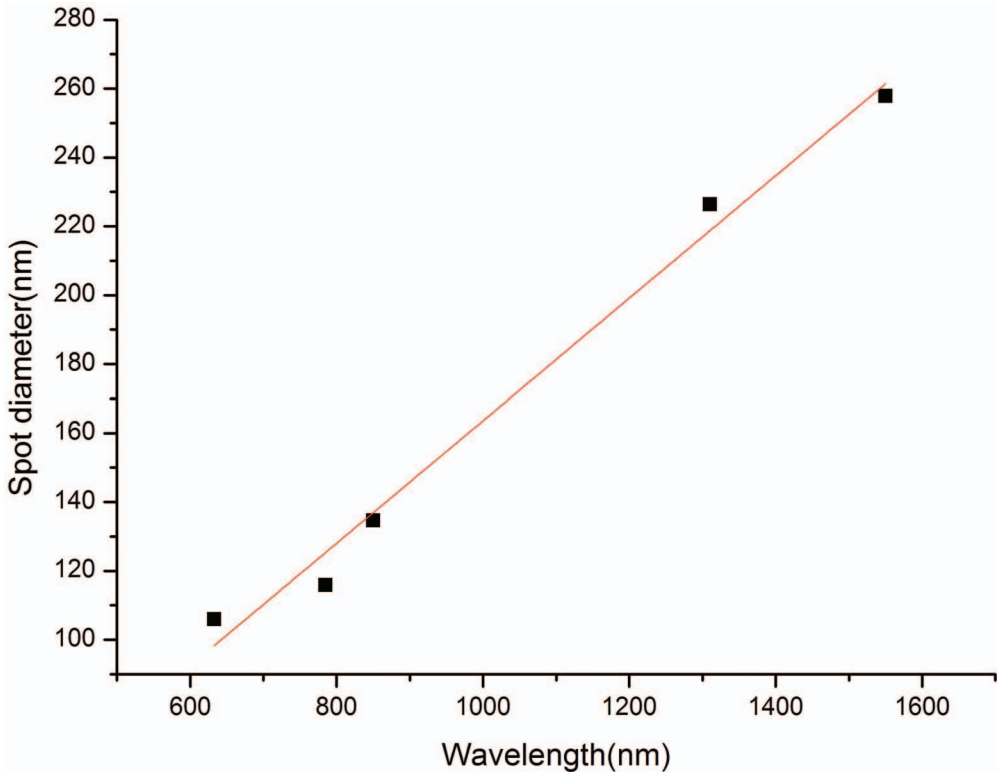

FIG. 4. the equivalent diameter of the light spot as a function of incident wavelength. The red solid line is the linear fitting result.

disorder is at about 8%, the enhancements reach the maximum. The enhancement factor can reach 16.5 for 785 nm and 23 for 850 nm, respectively.

Figure 6 showed the equivalent diameters of the light spots at different degrees of disorder when $\lambda = 785\ nm$, $r = 49\ nm$, $a = 204\ nm$, and $L = 3\lambda$. It is easy to get that the equivalent diameter of the light spot is almost a constant while increasing the degree of disorder. So we can conclude that the degrees of disorder have little effect on the light spot size.

In Figure 7, the degree of disorder w is 8%, $r = 49\ nm$, $a = 204\ nm$, $L = 3\lambda$. With the wavelength increasing, the equivalent spot diameter increases. From the results in Figure 6 and Figure 7 the size

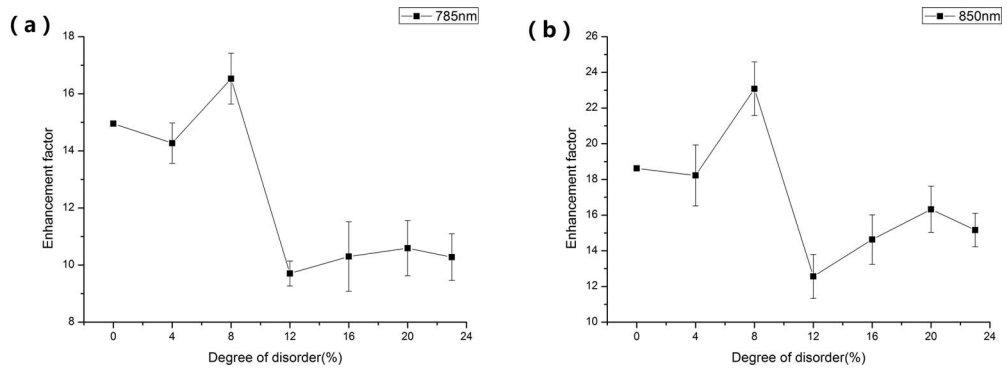

FIG. 5. The enhancements with different disorder degrees and at two incident wavelengths: (a) 785 *nm*. The parameters of the structure are $r = 49$ *nm*, $a = 204$ *nm*, and $L = 3\lambda$. (b) 850 *nm*. The parameters of the structure are $r = 53$ *nm*, $a = 222$ *nm*, and $L = 3\lambda$.

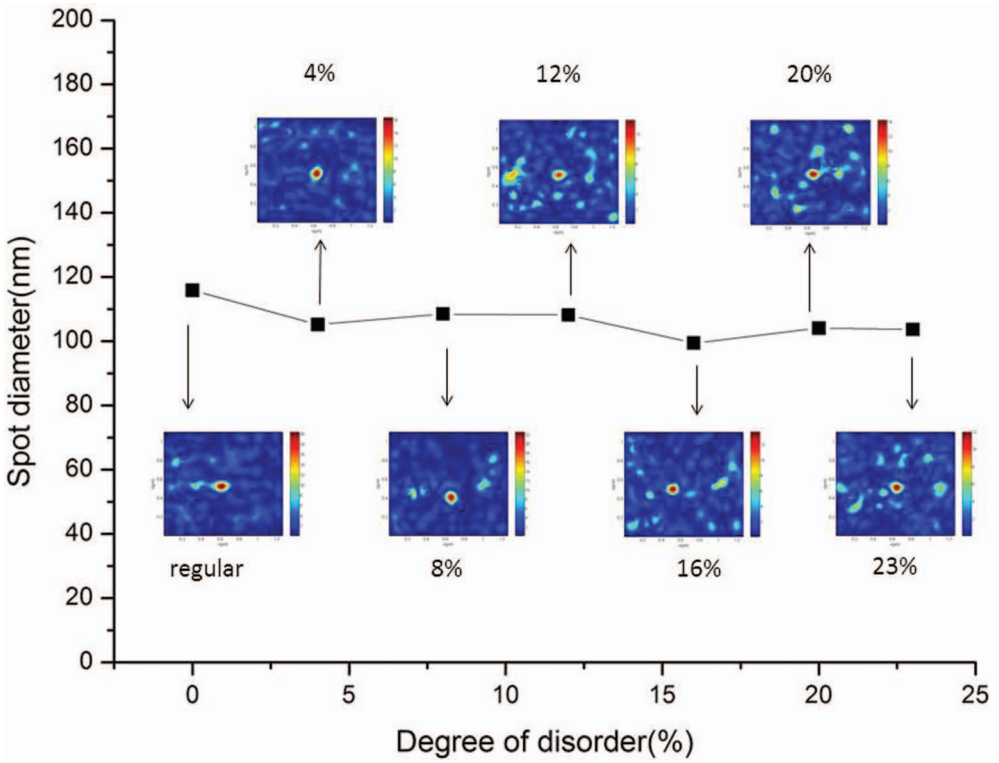

FIG. 6. The equivalent diameters of the light spot as a function of different disorder degrees. The structure parameters: $r = 49$ *nm*, $a = 204$ *nm*, and $L = 3\lambda = 2355$ *nm*. The incident wave wavelength is $\lambda = 785$ *nm*. The insets are the average intensity distribution $\overline{I}_R$ in the transverse section close to the output plane in each sample.

of the light spot is mainly depended on the incident wavelength in the same sample. The equivalent diameter of the light spot is approximate to $\lambda/7$, which is comparable to $\lambda/2n$.

IV. SUMMARY

In this paper, the properties of light localization in silicon nanostructure material with a triangular lattice of air holes (the lattice contains a cavity in the center) have been investigated by using the FDTD method. Numerical results in rigorous regular nanostructure showed that localization occurs and energy enhancement factor can reach 15 for 785 nm and 18.5 for 850 nm in the region of the

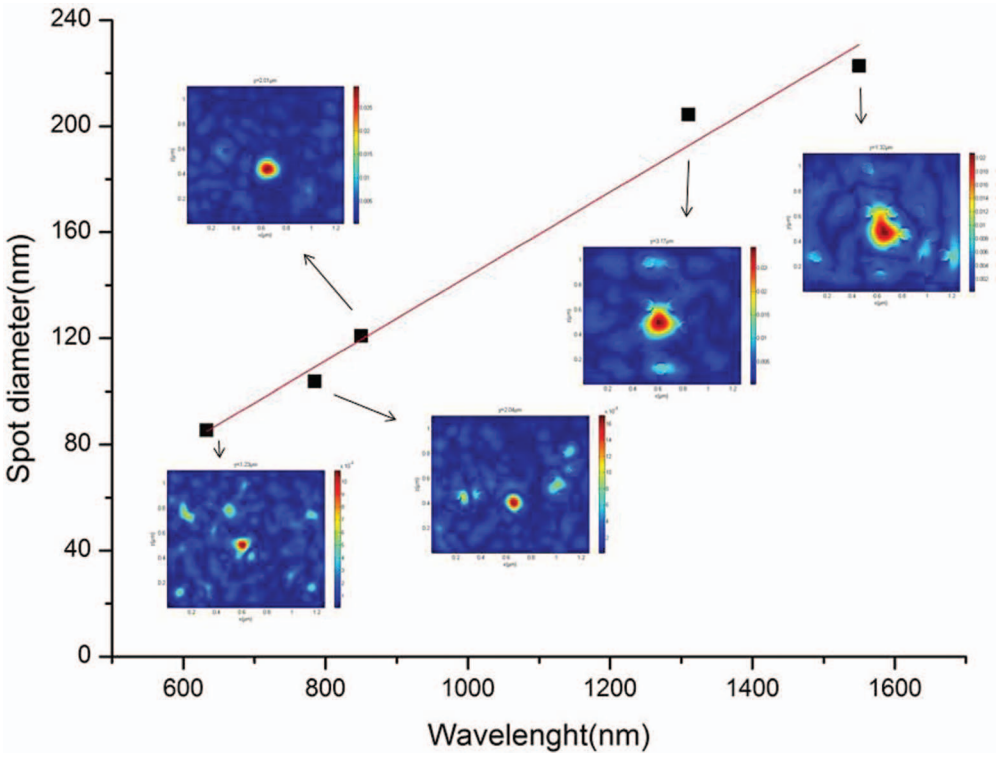

FIG. 7. The equivalent diameters of the light spot at different incident wavelengths in the structure with $r = 49\ nm$, $a = 204\ nm$, and $L = 3\lambda$. The degree of disorder is fixed as 8%. The insets are the average intensity distribution $\overline{I}_R$ in the transverse section close to the output plane at each wavelength.

cavity in specific structure. After adding perturbations to the positions of the holes, the localization effects at small degree of disorder ($< 5\%$) are similar to that in the homogeneous structure. The maximum enhancement of energy flux density appears at $w = 8\%$, the enhancement factor can reach 16.5 for 785 nm and 23 for 850 nm in the cavity. The results also showed that the disorder degrees have little influence on the size of localized spot. The size of the light spot is mainly depended on the incident wavelength in every sample and is approximate to $\lambda/7$.

So the structure we've studied in this paper can be used for additional enhancement of optical signals in silicon nanomaterials, besides the effects of enhanced Raman scattering from single silicon nanowires and SERS. On the other hand, detailed numerical study in a smaller range would help the understanding of more delicate mechanism of Anderson Localization in asymmetrical spatial nanophotonics, which will enable us to manipulate the photonic structure for different demands, and this would turned out to be of promising prospect of application in silicon-based photonics and optoelectronics.

ACKNOWLEDGMENTS

This project is supported by National Natural Science Foundation of China for research grants 11074131, National Science Fund for Talent Training in Basic Sciences under Grant No. J1103208. The author Yuanbin Wu wishes to thank Yanfang Liu for her help and support.

[1] P. E. Wolf and G. Maret, Phys. Rev. Lett. **55**, 2696 (1985).
[2] P. Sheng, "Introduction to wave scattering, localization and mesoscopic phenomena" (2006).
[3] M. P. V. Albada and A. Lagendijk, Phys. Rev. Lett. **55**, 2692 (1985).
[4] D. S. Wiersma, M. P. van Albada, and A. Lagendijk, Phys. Rev. Lett. **75**, 1739 (1995).
[5] A. Lagendijk, B. van Tiggelen, and D. S. Wiersma, Phys.Today **62**, 24–29 (2009).

[6] E. Yablonovitch, T. J. Gmitter, K. M. Leung, E. Gmitter, T. J. Leung, "Photonic band structure: the face-centered-cubic case employing nonspherical atoms," Phys. Rev. Lett. **67**(17), 2295–2298 (1991).
[7] T. F. Krauss, R. M. DeLaRue, S. Brand, "Two-dimensional photonic-bandgap structures operating at near-infrared wavelengths," Nature **383**(6602), 699–702 (1996).
[8] E. Yablonovitch, "Inhibited Spontaneous Emission in Solid-State Physics and Electronics," Phys. Rev. Lett. **58**(20), 2059–2062 (1987).
[9] V. P. Bykov, "Spontaneous Emission in a Periodic Structure," Soviet Journal of Experimental and Theoretical Physics **35**, 269–273 (1972).
[10] V. P. Bykov, "Spontaneous emission from a medium with a band spectrum," Quantum Electronics **4** (7), 861–871 (1975).
[11] Y. Qiu, H. C. Hao, J. Zhou, M. Lu, "A close to unity and all-solar-spectrum absorption by ion-sputtering induced Si nanocone arrays," Optics Express **20**, 22087 (2012).
[12] J. W. S. Rayleigh, "On the remarkable phenomenon of crystalline reflexion described by Prof. Stokes," Phil. Mag **26**, 256–265 (1888).
[13] K. Ohtaka, "Energy band of photons and low-energy photon diffraction," Physical Review B **19**(10), 5057–5067 (1979).
[14] M. Kashiwagi, K. Saitoh, K. Takenaga, S. Tanigawa, S. Matsuo, and M. Fujimaki, "Effectively single-mode all-solid photonic bandgap fiber with large effective area and low bending loss for compact high-power all-fiber lasers," Optics Express **20**, 15061 (2012).
[15] Z. Cao, X. Y. Qi, X. Q. Feng, Z. Y. Ren, G. Q. Zhang, and J. T. Bai, "Light controlling in transverse separation modulated photonic lattices," Optics Express **20**, 19119 (2012).
[16] B. Ung, A. Mazhorova, A. Dupuis, M. Rozé, and M. Skorobogatiy, "Polymer microstructured optical fibers for terahertz wave guiding," Optics Express **19**, B848 (2011).
[17] Review: S. Johnson (MIT) Lecture 3: Fabrication technologies for 3d photonic crystals.
[18] B. Alvaro, C. Emmanuel, G. Serguei, I. Marta, L. Stephen, W. L. Cefe, M. Francisco *et al.*, "Large-scale synthesis of a silicon photonic crystal with a complete three-dimensional bandgap near 1.5 micrometres," Nature **405**(6785), 437–440 (2000).
[19] Mathias Kolle, *Photonic Structures Inspired by Nature*, 5th ed. (2011), ISBN 978-3-642-15168-2.
[20] M. H. Bartl *et al.*, "Discovery of a diamond-based photonic crystal structure in beetle scales," Phys. Rev. Lett. **77**(5) 050904(R) (2008).
[21] T. Sakamoto, T. Mori, T. Yamamoto, L. Ma, N. Hanzawa, S. Aozasa, K. Tsujikawa, and S. Tomita, "Transmission over large-core few-mode photonic crystal fiber using distance-independent modal dispersion compensation technique," Optics Express **19**, B478 (2011).
[22] J. Ouellette, "Seeing the Future in Photonic Crystals," The Industrial Physicist **7**(6), 14–17 (DECEMBER 2001/JANUARY 2002).
[23] S. Godefroo, M. Hayne, M. Jivanescu, A. Stesmans, M. Zacharias, O. I. Lebedev, G. Van Tendeloo, and V. V. Moshchalkov, Nature Nanotechnology **3**, 174 (2008).
[24] M. R. Gartia, Y. Chen, and G. L. Liu, Appl. Phys. Rev. Lett. **99**, 151902 (2011).
[25] P. W. Anderson, Phil. Mag. B **52**, 505–509 (1985).
[26] S. Karbasi, C. R. Mirr, R. J. Frazier, P. G. Yarandi, K. W. Koch, and A. Mafi, "Detailed investigation of the impact of the fiber design parameters on the transverse Anderson localization of light in disordered optical fibers," Optics Express **20**, 18692 (2012).
[27] T. Schwartz, G. Bartal, S. Fishman, and M. Segev, Nature (London) **446**, 52 (2007).
[28] C. Conti and A. Fratalocchi, Nature Physics **14**, 794 (2008).
[29] L. Martin, G. D. Giuseppe, A. Perez-Leija, R. Keil, F. Dreisow, M. Heinrich, S. Nolte, A. Szameit, A. F. Abouraddy, D. N. Christodoulides, and B. E. A. Saleh, Optics Express **19**, 13636 (2011).
[30] B. A. van Tiggelen, Phys. Rev. Lett. **75**, 422 (1995).
[31] A. Sparenberg, G. L. J. A. Rikken, and B. A. van Tiggelen, Phys. Rev. Lett. **79**, 757 (1997).
[32] F. Scheffold and G. Maret, Phys. Rev. Lett. **81**, 5800 (1998).
[33] D. S. Wiersma, M. Colocci, R. Righini, and F. Aliev, Phys. Rev. B **64**, 144208 (2001).
[34] G. Fujii, T. Matsumoto, T. Takahashi, and T. Ueta, "Study on transition from photonic-crystal laser to random laser," Optics Express **20**, 7300 (2012).
[35] A. C. T. Thijssen, M. J. Cryan, J. G. Rarity, and R. Oulton, "Transfer of arbitrary quantum emitter states to near-field photon superpositions in nanocavities," Optics Express **20**, 22412 (2012).
[36] A. Taflove and S. C. Hagness, *Computational Electrodynamics: the Finite-Difference Time-Domain Method*, 3rd ed. (Artech House, 2000).
[37] L. Y. Cao, B. Nabet, and J. E. Spanier, Phys. Rev. Lett. **96**, 157402 (2006).
[38] Y. B. Wu, Y. F. Wang, and X. W. Cao, J. Appl. Phys. **105**, 023103 (2009).
[39] Y. B. Wu, Y. F. Wang, and X. W. Cao, J. Appl. Phys. **106**, 053106 (2009).
[40] D. E. Aspnes and A. A. Studna, Phys. Rev. B **27**, 985 (1983).